Saudi Pharmaceutical Journal 31 (2023) 335–347

HOSTED BY

Contents lists available at ScienceDirect

Saudi Pharmaceutical Journal

journal homepage: www.sciencedirect.com

Original article

Superporous hydrogels based on blends of chitosan and polyvinyl alcohol as a carrier for enhanced gastric delivery of resveratrol

Ousanee Issarachot [a,b], Suputra Bunlung [a,c], Kanidta Kaewkroek [d], Ruedeekorn Wiwattanapatapee [a,c,*]

[a] Department of Pharmaceutical Technology, Faculty of Pharmaceutical Sciences, Prince of Songkla University, Songkhla 90110, Thailand
[b] Pharmacy Technician Department, Sirindhron College of Public Health of Suphanburi, 77 moo4, Tubteelek sub-district, Mueang district, Suphanburi 72000, Thailand
[c] Phytomedicine and Pharmaceutical Biotechnology Excellence Research Center, Faculty of Pharmaceutical Sciences, Prince of Songkla University, Hat-Yai, Songkhla 90110, Thailand
[d] Faculty of Integrative Medicine, Rajamangala University of Technology Thanyaburi, Thanyaburi, Pathum Thani 12130, Thailand

ARTICLE INFO

Article history:
Received 12 October 2022
Accepted 2 January 2023
Available online 5 January 2023

Keywords:
Superporous hydrogel
Resveratrol
Chitosan
Gastro-retentive drug delivery system

ABSTRACT

Resveratrol exhibits a number of pharmacological properties, notably antioxidant, anti-inflammatory and anti-cancer activities which are beneficial for the treatment of gastric diseases. However, the poor aqueous solubility and rapid metabolism are the important limitations in clinical uses. Superporous hydrogels (SPHs) based on chitosan/PVA blends were developed as a carrier for resveratrol solid dispersion (Res_SD) to increase the solubility and achieve sustained drug release in the stomach. The SPHs were prepared by gas forming method using glyoxal and sodium bicarbonate as cross-linking agent and gas generator, respectively. The solid dispersions of resveratrol with PVP-K30 were prepared by solvent evaporation and incorporated into the superporous hydrogels. All formulations showed rapid absorption of simulated gastric fluid and reached the equilibrium swollen state within a few minutes. The water absorption ratio and mechanical strength of SPHs were predominantly affected by the chitosan content, with maximum values at 1400 % and 375 g/cm^2, respectively.

The Res_SD-loaded SPHs exhibited good floating properties and SEM micrographs revealed a highly interconnected pores structure with size around 150 μm. Resveratrol was efficiently entrapped within the SPHs at levels between 64 and 90 % w/w and efficient drug release was sustained over 12 h dependent on the concentration of chitosan and PVA. The Res_SD-loaded SPHs exhibited slightly less cytotoxic effect towards AGS cells than pure resveratrol. Furthermore, the formulation showed similar anti-inflammatory activity against RAW 264.7 cells compared with indomethacin.

1. Introduction

Gastro-retentive drug delivery systems (GRDDS) have been investigated extensively to overcome the disadvantages of conventional oral dosage forms. GRDDS are designed to prolong gastric residence time by several mechanisms including floating on the gastric content, swelling/expansion, bioadhesion and the use of high density systems (Nayak et al., 2010; Tripathi et al., 2019). The aims are to enhance the bioavailability of narrow absorption window drugs and avoid rapid metabolism through sustained drug release in the stomach. Moreover, GRDDS are normally advocated for specific treatment of conditions arising in the stomach (Omidian and Park, 2011).

Superporous hydrogel (SPH) makes up one type of GRDDS that exhibits rapid swelling in a few minutes due to the interconnected pores network within the gel structure which subsequently leads to the systems with larger dimensions than the pylorus sphincter (Kumari et al., 2020; Omidian and Park, 2011). Numerous SPH formualtions have been developed in attempts to optimise mechanical strength, swelling and drug release behavior, based on a variety of different types of polymers including poly(acrylic acid-*co*-acrylamide), sodium alginate, sodium carboxymethyl cellulose and chitosan (Chavda et al., 2009; Omidian et al., 2007). Among these polymers, chitosan, a natural polymer produced from deacetylation of chitin has been widely investigated for production of GRDDS due to its favourable biodegradability and biocompatibility. In addition, the swelling behavior and stability of chitosan SPH may be enhanced by crosslinking of gel formations. Further

* Corresponding author.
E-mail address: ruedeekorn.w@psu.ac.th (R. Wiwattanapatapee).
Peer review under responsibility of King Saud University.

Production and hosting by Elsevier

https://doi.org/10.1016/j.jsps.2023.01.001
1319-0164/

improvements in the mechanical properties of SPHs have been demonstrated following incorporation of hydrophilic polyvinyl alcohol (PVA), as an auxillary polymer during preparation of chitosan superporous hydrogels (Omidian et al., 2007).

Resveratrol (Res), a phenolic compound, obtained from various plants such as grapes and berries has been reported to display antioxidant, cardioprotective, neuroprotective, anti-inflammatory and anticancer activities (Kuršvietienė et al., 2016; Ko et al., 2017; Yang et al., 2018). Resveratrol has been shown to prevent gastric cancer cell growth by suppressing MALAT1 expression and inhibit gastric inflammation caused by *Helicobacter pylori* (Zhang et al., 2015; Yang et al., 2018; Pannu and Bhatnagar, 2019). In addition, it was found that low doses of resveratrol could inhibit human gastric cancer cell invasion by blocking the IL-6 induced Raf-MAPK pathway activation (Yang et al., 2018). Resveratrol has also been reported to induce both protective and therapeutic effects in the treatment of gastric ulcers by inhibiting pro-inflammatory cytokines (Solmaz et al., 2009).Although the potential advantages of resveratrol for treatment of a number of gastric conditions have been demonstrated, the efficacy of resveratrol is severely limited due to the poor aqueous solubility and rapid metabolism of the phenol *in vivo*. Several strategies have been used to improve the solubility and bioavailability of poorly water-soluble natural compounds, including micellar solubilization (Almeida et al., 2020), particle size reduction by micronization (Sachett et al., 2022), and self-emulsifying systems (Sermkaew et al., 2013; Jaisamut et al., 2017; Petchsomrit et al., 2017). Among these, solid dispersion (SD) is one of the most widely used methods because the preparation process is feasible, and suitable for scaling-up in industry (Sharma et al., 2019; Tran et al., 2019; Van den Mooter, 2012).

In recent years, various formulations of SPH have been investigated as platforms for sustained release of drug molecules in the stomach. These systems were successfully employed for water-soluble drugs such as ranitidine hydrochloride, rosiglitazone maleate and drotaverine hydrochloride (Chavda et al., 2010; Gupta and Shivakumar, 2010; Farag et al., 2022). By contrast, the application of gastro-retentive SPH with poorly water-soluble compounds have not been previously reported. Therefore, the gastro-retentive SPH systems merging with solid dispersion technology are developed in this study to increase the solubility, enhance the gastric residence time and prolong the release of a poorly water-soluble phenolic compound, resveratrol.

The main aim of this study was to develop gastro-retentive SPH based on chitosan/PVA blends in order to prolong the release of resveratrol for treatment of gastric disorders. The compound was first formulated as a solid dispersion with a hydrophilic carrier, polyvinylpyrolidone (PVP K-30), to improve solubility and dissolution behavior, prior to incorporation in the SPH. The Res_SD loaded SPH formulations were subsequently evaluated with respect to swelling ratio, mechanical strength, resveratrol entrapment efficiency and *in vitro* release. The cytotoxic activity of the developed formulation and wound healing effect were assessed using gastric epithelial cell line (AGS) and the anti-inflammatory activity was measured using murine macrophage cell line (RAW 264.7).

2. Materials and methods

2.1. Materials

Chitosan (Mw 300,000, degree of deacetylation 92 %) was purchased from Seafresh industry ltd. (Bangkok, Thailand). Resveratrol extract (purity ~ 98 %) was from Pioneer Herb.

Polyvinylpyrrolidone K30 (PVP-K30) was supplied by P.C. Drug Center Co., ltd. (Bangkok, Thailand). Glyoxal solution (40 %) and Polyvinyl alcohol (PVA, average molecular weight 30,000 – 70,000) were obtained from Sigma Co. (St. Louis, MO, USA). Dimethylsulfoxide (DMSO) was from Amrescov (OH, USA). All other chemical were of reagent grade and used as received without further purification.

The human gastric epithelial cancer cell line (AGS) and murine macrophage cell line (RAW264.7) were obtained from the American Type Culture Collection, ATCC (VA, USA). Fetal calf serum (FCS) was provided by Gibco (Invitrogen, California, USA). Penicillin-streptomycin was from Invitrogen (Invitrogen, California, USA). Lipopolysaccharide (LPS, from *Escherichia coli*), 3-(4,5-dimethyl-2-thiazolyl)-2,5-diphenyl-2H-tetrazolium bromide (MTT), Roswell Park Memorial Institue 1640 (RPMI-1640) medium, Dulbecco's modified Eagle's medium (DMEM), indomethacin and phosphate buffer saline (PBS) were obtained from Sigma Aldrich (Sigma Aldrich, Missouri, USA).

2.2. Preparation of resveratrol solid dispersion (Res_SD) and resveratrol physical mixture (Res_PM)

Solid dispersions of resveratrol and PVP-K30 were prepared by solvent evaporation using ethanol on account of ethanol's ability to completely dissolve both components and to be easily removed without harmful residue (Kerdsakundee et al., 2015; Zhang et al., 2018). Following dissolution of resveratrol and PVP-K30 (weight ratios 1:1, 1:3, 1:6 and 1:9), the solvent was removed by rotary evaporation at 40 °C under reduced pressure to obtain dried solid, which was subsequently ground and passed through a sieve (250 μm). Physical mixture of resveratrol and PVP-K30 in the same weight ratios for preparation of solid dispersions were mixed and passed through a 250 μm sieve. Res_SD and Res_PM formulations were stored in a desiccator and protected from light.

2.3. Solubility and dissolution studies of Res_SD and Res_PM

Solubility studies were conducted using the flask shaking method (Kerdsakundee et al., 2015). Briefly, an excess amount of each Res_SD or Res_PM preparation was added to a tube containing 1 mL of 0.1 N HCl and mixed vigorously by vortex mixer. The sample tubes were transferred to a shaker bath (37 ± 0.1 °C, 100 rpm) for 48 h. The test samples were then centrifuged (Hettich Zentrifugen D-78532 Tuttlingen Model 16R, Germany) at 4 °C, 6,000 rpm for 60 min and the supernatant was collected and filtered through a 0.45 μm filter (VertiPure^{TM} PVDF(HL), Vertical Chromatography Co., ltd., Bangkok, Thailand). The concentration of resveratrol in the supernatant was analyzed at 306 nm using UV–vis spectroscopy by comparison with a calibration curve prepared using series dilution of resveratrol in 0.1 N HCl. Each Res_SD and Res_PM preparation was analyzed in triplicate.

The release behavior of resveratrol from Res_SD and Res_PM preparations was investigated using the USP dissolution apparatus II (paddle speed 50 rpm, 900 mL of 0.1 N HCl (pH 1.2) dissolution medium, 37 °C ± 0.5 °C (Kerdsakundee et al., 2015). Samples (5 mL) were withdrawn after 5, 10, 15, 30, 45, 60, 90 and 120 min and the same volume of fresh dissolution medium was added. The amount of resveratrol released were analyzed by UV–vis spectroscopy at 306 nm as described above and each formulation was tested in triplicate.

2.4. Preparation of Res_SD loaded superporous hydrogel (Res_SD SPH)

The components of Res_SD SPH formulations are shown in Table 1. Res_SD SPHs were prepared by a gas foaming method as described earlier with some modification (Chavda et al., 2009; Gupta and Shivakumar, 2010). Chitosan was employed as the hydrogel forming polymer whereas PVA was used to enhance the

Table 1
Components of Res_SD loaded SPH formulations.

Formulation	Chitosan soln. (% w/v)	PVA soln. (% w/v)	10 % Glyoxal soln. (% v/v)	$NaHCO_3$ (mg)	Res_SD (mg)
Effect of chitosan content					
F1	0.5	0.5	0.50	50	100
F2	1	0.5	0.50	50	100
F3	1.5	0.5	0.50	50	100
F4	2	0.5	0.50	50	100
Effect of PVA content					
F5	1	0	0.50	50	100
F6	1	0.50	0.50	50	100
F7	1	1.00	0.50	50	100
F8	1	2.00	0.50	50	100
Effect of glyoxal solution					
F9	1	0.5	0.00	50	100
F10	1	0.5	0.25	50	100
F11	1	0.5	0.50	50	100
F12	1	0.5	1.00	50	100
Effect of Res_SD content					
F13	1	0.5	0.50	50	100
F14	1	0.5	0.50	50	200
F15	1	0.5	0.50	50	300
F16	1	0.5	0.50	50	400

*F2,F6,F11,F13 were the same formulations.

strength of polymer network within the gel. Chitosan and PVA were weighed and co-dissolved in 5 mL of acetic acid solution (3 % v/v) to yield the concentrations listed in Table 1. Glyoxal solution (10 % w/v) and Res_SD were added into the co-polymer solution, and mixed by stirrer until a uniform mixture was obtained. Finally, sodium bicarbonate was added as a porogen to create a pore structure within the hydrogel together with gelation process. The resulting Res_SD SPH preparations were poured into 24 well-plates and placed at 5 °C overnight. The freezed hydrogels were further lyophilized (Freeze dryer). The dried materials were stored in a desiccator. The content of chitosan, PVA, glyoxal solution and Res_SD were systematically varied to optimize physicochemical characteristics.

2.5. Water absorption capacity and density measurement of Res_SD SPH

The water absorption capacity of dried Res_SD SPH (based on weight gain) was monitored in 0.1 N HCl (pH 1.2) on a 2 h period. At predetermined time intervals, the swollen sample was removed from the medium and carefully placed on a sieve to remove excess fluid, prior to weighing. The water absorption capacity was calculated using triplicate samples of each preparation according to equation (1).

$$Water\ absorption\ capacity = (Ms - Md/Md) * 100 \quad (1)$$

where Ms is the weight of Res_SD SPH in the swollen state and Md is the weight of dried Res_SD SPH.

The density of dried Res_SD SPHs was determined by the solvent displacement method (Chavda and Patel, 2010). Samples in triplicate were weighed and each was placed in a graduated cylinder containing hexane. The density of Res_SD SPHs was calculated using equation (2).

$$Density = m/v \quad (2)$$

where m is mass of dried Res_SD SPHs and v is incremental increase in hexane volume.

2.6. Compressive strength measurement

The compressive strength of Res_SD SPHs was measured according to previous report with minor modification using a Stable Micro Systems Texture Analyzer (Texture Technologies Corp Scarsdale, NY) (Gupta and Shivakumar, 2010). Dried SPH samples in the cylindrical shape were swollen to the equilibrium state by immersion in 0.1 N HCl and placed on the loading platform of the Texture Analyzer. The test samples were comprssed using a stainless steel cylindrical probe under conditions of the pre-test speed (2.0 mm/*sec*), test speed (1.0 mm/*sec*) and post-test speed (2.0 mm/*sec*) and the maximum load was recorded. Each Res_SD SPH preparation was tested in triplicate.

2.7. Determination of resveratrol content of Res_SD SPH

The content of resveratrol in each Res_SD SPH preparation was determined by immersing 30 mg samples in methanol overnight. The solution was filtered through paper filter (Whatman® No. 1) and diluted with methanol to obtain suitable concentrations for analysis by UV spectrophotometry as described in section 2.3. Each formulation was done in triplicate.

2.8. FT-IR studies

FTIR spectroscopy was carried out using a PerkinElmer spectrum 400 (FTIR spectrometer shimadzu, Kyoto, Japan). Samples were prepared by compressing to KBr disc and scanned over the range 3000–500 cm^{-1} to identify functional groups within the Res_SD SPH and resveratrol/excipient interactions.

2.9. X-ray diffraction (XRD)

X-ray powder diffraction was performed using X-ray diffractometer (model D-5005 diffractometer, Siemens AG, Munich, Germany). The diffraction pattern was analyzed at angles 2θ from 2 to 50° with an angle variation of 0.02°/s while applying 40 kV and 0.3 A.

2.10. Thermal analysis

The thermal behavior of dried Res_SD SPH preparations was examined using differential scanning calorimetry (DSC). Analysis was performed at a heating rate of 10 °C min^{-1} over the temperature range 30 °C to 250 °C under a nitrogen atmosphere (Perkin Elmer, DTA7, USA).

2.11. Morphological investigations

The porous structure of dried SPHs was investigated by scanning electron microscopy (SEM) (Quanta 400, Hitachi, Tokyo, Japan). Samples were immersed in liquid nitrogen and cross-sectioned to expose their internal structure. The inner surface of the dried hydrogels was coated with a thin layer of gold alloy using Sputter coater prior to examination in the SEM at an operating voltage of 10 kV.

2.12. In vitro release of resveratrol from Res_SD SPH

The release behavior of resveratrol from Res_SD SPH formulations was investigated using the USP dissolution apparatus II (paddle speed 75 rpm, 900 mL of 0.1 N HCl (pH 1.2) dissolution medium, 37 °C ± 0.5 °C (Kerdsakundee et al., 2015). Samples (5 mL) samples were collected at 30, 45 min and 1, 1.5, 2, 4, 6, 8, 12 h and the same volume of fresh dissolution medium was added.The amount of resveratrol released were analyzed by UV–vis spectroscopy at 306 nm as previously described in section 2.3 and each formulation was tested in triplicate.

2.13. Weight loss of Res_SD SPH in simulated gastric fluid

The weight loss of SPHs was investigated under the same experimental conditions described above (section 2.12) for release testing of resveratrol (Qiu and Park, 2003). Dried SPH samples were placed in the dissolution vessel and removed at predetermined times. Then, the SPHs were dried in a hot air oven at 40 °C and weighed to determine the % weight remaining using the following equation.

$$\%remaining\ weight = [(Wt - Wi)/Wi]\ x100 \quad (3)$$

where Wi is the initial dry weight of SPHs and Wt is the dry weight at time t.

2.14. In vitro cytotoxicity

The *in vitro* cytotoxicity of Res_SD SPH preparations was assessed using the MTT assay in combination with the human gastric epithelial cancer cell line (AGS) as previously described (Kaewkroek et al., 2022). Cells were cultured in DMEM supplemented with 10 % FBS, 1 % penicillin–streptomycin solution, 0.1 % human insulin, and 1 % sodium pyruvate. AGS cells were seeded at a density of $2x10^4$ cells/well in a 96-well plate and incubated at 37 °C under 5 % CO_2 atmosphere for 24 hr. Subsequenly, the medium was removed and the cells were washed with serum-free medium prior to exposure to various concentrations of a) Res_SD SPH, b) blank SPH, c) Res_SD and d) pure resveratrol diluted with serum-free medium for 24 h. The cells were subsequently treated with MTT solution and further incubated for 3 h. At the designated time interval, the MTT solution was removed and the formazan crytals produced in viable cells were dissolved using DMSO. The optical density was measured at 570 nm by a microplate reader (SPECTROstar Nano, BMG LABTECH, Ortenberg, Germany) and culture medium was used as control. The % cell viability was calculated using the following equation:

$$\%viability = [ODsample/ODcontrol] * 100 \quad (4)$$

2.15. Anti-inflammatory activity

The anti-inflammatory activity of Res_SD SPH preparations was evaluated by measuring the inhibition of nitric oxide (NO) production in RAW264.7 cells (Kaewkroek et al., 2022). The cells were cultured in RPMI 1640 medium supplemented with sodium bicarbonate 0.1 % and glutamine, penicillin G 2 mM (100 units/mL), streptomycin (100 μg/mL) and 10 % fetal calf serum (FCS). Cells were seeded at a density of $1x10^5$ cells/well in a 96-well plate and incubated at 37 °C under 5 % CO_2 atmosphere for 1 h. The culture medium was removed and replaced with a mixture of LPS and Res_SD SPH test samples in serum free medium for 24 h. The level of NO production was determined be assay of the amount of nitrile in the culture medium using Griess reagent. The optical density was measured at 570 nm using a microplate reader.

2.16. Wound healing assay

In vitro wound healing assay was investigated using an AGS cell line to measure collective cell migration as previously report (Wannasarit et al., 2019; Kaewkroek et al., 2022). Cells were seeded at a density of $4x10^4$ cells/well in a 6-well plate for 24 h using DMEM supplemented with 10 % FBS and 1 % penicillin/streptomycin as cultred medium. After reaching a confluent monolayer, the cells were washed with PBS and fixed with 3.7 % paraformaldehyde for 30 min. The fixed cells were stained with 1 % crystal violet in 2 % ethanol for a further 30 min. A wound gap was created using a sterile scratcher (0.5 mm, SPL life Sciences, Gyeonggi-do, Korea). Samples of Res_SD SPH were diluted with serum free medium to the equvanet concentration of resveratrol at 10 μg/ml. Then, the samples were added to the wells and narrowing of the wound gap was monitored after 24 h. Photographs of the wound gap before and after addition of Res_SD SPH test ssamples were recorded using phase contrast microscopy (Nikon Instrumentals Inc., New York, USA).

The percentage relative wound closure was calculated using the following equation:

$$\%relative\ wound\ closure = [(A_i - A_t)/A_i]x100 \quad (5)$$

When A_i is initial area of wound gap after scratching, A_t is area of wound gap at 24 h.

2.17. Statistical analysis

Data were presented as mean values ± standard deviation (SD). Significant of differences were evaluated using Student's *t*-test and one-way ANOVA with p values<0.05 considered statistically significant.

3. Results and discussion

3.1. Characterization of resveratrol solid dispersions (Res_SD) and resveratrol physical mixture (Res_PM)

Solid dispersions of resveratrol and PVP-K30 at various w/w ratios were successfully prepared by solvent evaporation using ethanolic co-solutions. The ratio of Res and PVP-K30 was confined to 1:3 to 1:9 since use of a lower ratio at 1:1 resulted in formation of a viscous mixture following solvent evaporation instead of dried powder. PVP-K30 was selected as the hydrophilic carrier since the polymer is non-crystalline and has been shown previously to be advantageous for preparing solid dispersion of phenolic compounds such as curcumin (Kaewnopparat et al., 2009; Kerdsakundee et al., 2015; Liang et al., 2007). Moreover, solid dispersions based on PVP-K30 have demonstrated an ability to inhibit drug precipitation in gastrointestinal environment. Res_SD and Res_PM were characterized in terms of solubility, *in vitro* dissolution release, release behavior, XRD, DSC and FI-IR as follows.

3.1.1. Solubility of Res_SD and in vitro dissolution studies

Solubility enhancement of poorly water-soluble drugs is a major challenge for development of effective medicines from such entities. In the present study, resveratrol demonstrated low solubility of 0.12 mg/mL in 0.1 N HCl at 37 °C but the solubility increased significantly by a factor of 10 using simple (1:9) physical mixtures with PVP-K30 (Table 2). The production of resveratrol solid dispersions with PVP-K30 also resulted in increased solubility with increasing content of PVP but the higher ratio of 1:9 produced a remarkable enhancement of resveratrol solubility of approximately 500 fold (61.50 ± 0.170 mg/mL). The lower ratio of resveratrol to PVP (1:3) was not effective in elevating solubility in SD or physical mixture form. Explanations for the enhanced solubility of resveratrol in solid dispersions featuring high PVP content have been explained in previous study (Gao and Shi, 2012). High concentrations of hydrophilic polymers tend to enhance the transformation of crystalline drug form to amorphous form resulting in increased solubility of resveratrol by specific interaction between drug and polymer including hydrogen bond formation and ionic interaction (Gao and Shi, 2012; Huang and Dai, 2014; Fitriani et al., 2016).

3.1.2. Powder X-ray diffraction studies (XRD)

Resveratrol displayed distinct peaks at 2Θ angles of 2.50, 16.37, 19.19, 22.36, 26.69 and 28.30 in the X-ray diffractogram (Fig. 1A) corresponding to the crystalline form. No peaks were observed in PVP-K30 XRD spectra (Fig. 1B) indicating the amorphous form of the carrier. All Res_PMs (1:3 to 1:9 wt ratio) retained the dominant crystalline peaks at the same 2Θ positions as resveratrol. In contrast, the resveratrol solid dispersions with PVP-K30 displayed only the broaden peaks of PVP-K30 indicating the transition of crystalline resveratrol to the amorphous form in the solid dispersion. This behavior is explained by interference of the PVP carrier polymer with crystal nucleation and growth-processes of resveratrol, resulting in precipitation in amorphous form during solvent evaporation. Another possible explanation involves inhibition of crystal nucleation in solution due to resveratrol-PVP interaction via hydrogen bonding (Wegiel et al., 2013).These mechanisms of crystallization inhibition are excluded in simple mixtures of drug and carrier.

3.1.3. Differential scanning calorimetry

DSC thermograms of resveratrol, PVP-K30, Res_SDs and Res_PMs are illustrated in Fig. 2. Resveratrol revealed a sharp endothermic peak at around 266 °C, corresponding to the crystal melting point of resveratrol whereas no peak was observed for PVP-K30 indicating its amorphous state. No resveratrol melting peak was observed for Res_SD samples, suggesting that the resveratrol component exists in amorphous form as evidenced by XRD results (Section 3.1.2). No endothermic peaks were recorded for Res_PMs which may be explained by dissolution of resveratrol in molten PVP-K30 phase during thermal analysis as mentioned in other studies (Baghel et al., 2016).

Table 2
The solubility of non-formulated resveratrol, resveratrol solid dispersion (Res_SD) and resveratrol physical mixture (Res_PM) with PVP-K30 in 0.1 HCl at 37 °C.

Sample	Solubility (mg/mL) (mean ± S.D)	Sample	Solubility (mg/mL) (mean ± S.D)
Resveratrol	0.12 ± 0.03		
1:3 PM	0.18 ± 0.01	1:3 SD	0.10 ± 0.01
1:6 PM	0.46 ± 0.09	1:6 SD	0.61 ± 0.02
1:9 PM	1.13 ± 0.03	1:9 SD	61.50 ± 0.17

3.1.4. FT-IR analysis

FT-IR spectra (Fig. 3) was performed to support the interaction between the absorption peak of the drug and polymer (Boontawee et al, 2022). The FT-IR spectrum of resveratrol showed peaks at 3234 cm^{-1} assigned to the hydroxyl (O—H) whereas PVP-K30 showed the absorption band at 1659 cm^{-1} attributed to the carbonyl group (C═O). FT-IR spectra recorded for 1:9 Res-SD showed the absorption band of carbonyl group group of PVP-K30 lower to 1600 cm^{-1}. This results indicated the interaction between resveratrol containing OH hydrogen bond donor groups, which allows hydrogen bond formation with a polymer containing an appropriate acceptor group such as C═O groups (Kerdsakundee et al., 2015; Fitriani et al., 2016; Boontawee et al., 2022). Such interactions including hydrophobic and electrostatic effects, may lead to improvements in drug solubility and dissolution behavior (Tran et al., 2019).

3.1.5. In vitro dissolution behavior

The *in vitro* dissolution profile of resveratrol, Res_SDs and Res_PMs in 0.1 N HCl (pH 1.2) are presented in Fig. 4. Resveratrol dissolution was restricted to<15 % within 2 h, due to the hydrophobicity and poor solubility of the phenol. Physical mixtures of resveratrol and PVP-K30 resulted in increasing resveratrol dissolution which increasing PVP content reaching a level of 42 % at 2 h for 1:9 Res_PM preparations.This behavior may be explained by increased wetting of the resveratrol particle component of the mixture by dissolved PVP. In the case of Res_SDs, resveratrol dissolution reached a miximum of 71 % for weight ratio 1:9 while the lower ratios of 1:3 and 1:6 were not effective in enhancing dissolution. The marked improvement in resveratrol dissolution with increasing content of PVP may be attributed to the transition of resveratrol to the amorphous state as discussed above, and would be expected to result in corresponding improvement in bioavailability and dose reduction of the drug *in vivo* (Afifi, 2015; Panizzon et al., 2019). Based on solubility and dissolution testing, Res_SD preparation of w/w ratio 1:9 were selected for loading into superporous hydrogels.

3.2. Characterization of Res_SD loaded SPHs

3.2.1. Preparation of SPHs

Resveratrol solid dispersions (Res_SD) were successfully incorporated in superporous hydrogels (SPH) using a gas foaming technique. Hydrogels were produced from chitosan as the main gel-forming polymer together with PVA as an auxillary polymer. Glyoxal solution was used as a crosslimking agent to increase the strength of the gel network. The pore structure was produced by sodium bicarbonate as a gas forming agent to the co-solution of chitosan and PVA in acetic acid after addition of the crosslinking agent. The resulting SPHs were freeze dried prior to detailed physicochemical characterization and evaluation of cytotoxicity, anti-inflammatory and wound healing capability in cell culture as follows.

3.2.2. Appearance, weight variation and density

Res_SD SPHs were produced in the form of cylindrical shape and exhibited white to yellowish color (Fig. 5). The average weight ranged from 210.2 to 361.8 mg depending on the polymer content and drug loading. SPHs displayed highly fluid absorption with slightly increase in dimensions after immersion in 0.1 N HCl (Fig. 5).

The apparent density of the various SPHs ranged from 0.112 ± 0.002 to 0.619 ± 0.128, which is lower than the density of gastric fluid (<1.004 g/mL) indicating that the SPH would float and remain in the stomach following oral dosing (Bhalla and Nagpal, 2013; Payghan, 2014).The SPHs density was affected significantly by

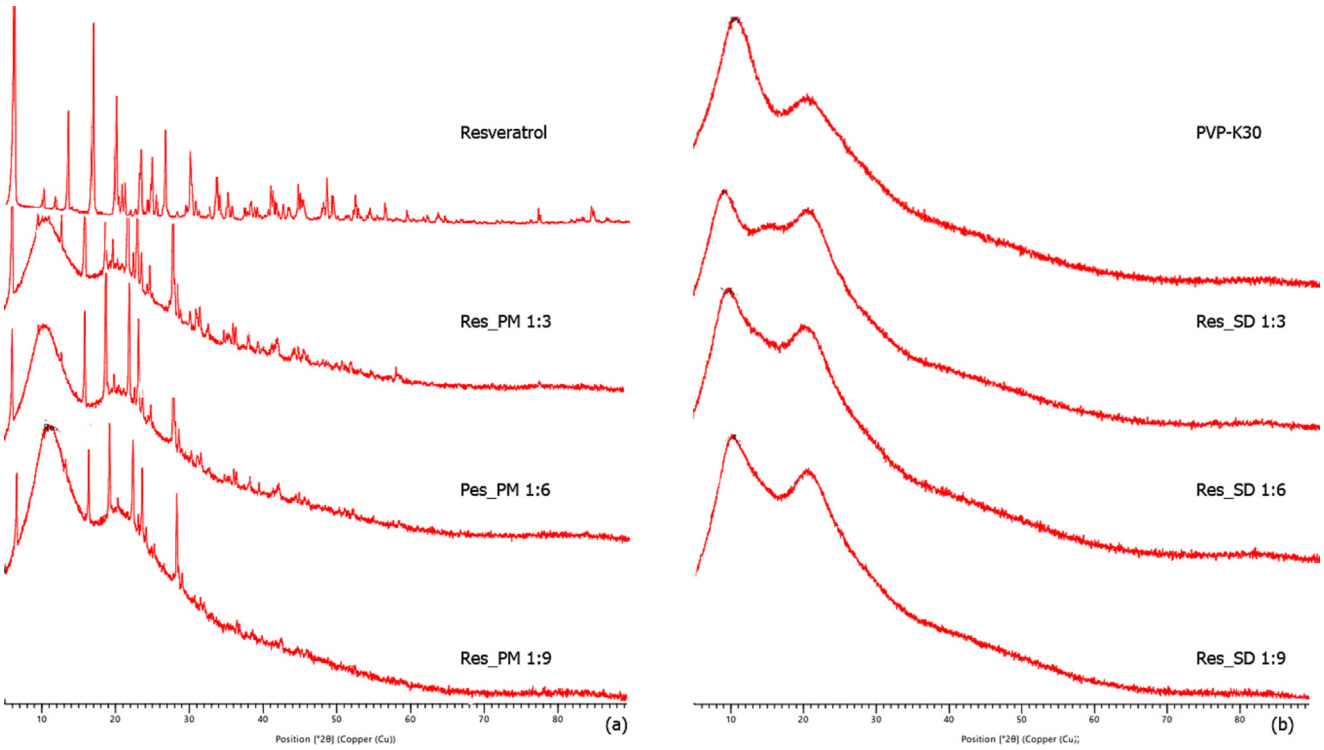

Fig. 1. XRD spectra of resveratrol, PVP-K30, resveratrol solid dispersion (Res_SD) and resveratrol physical mixture (Res_PM).

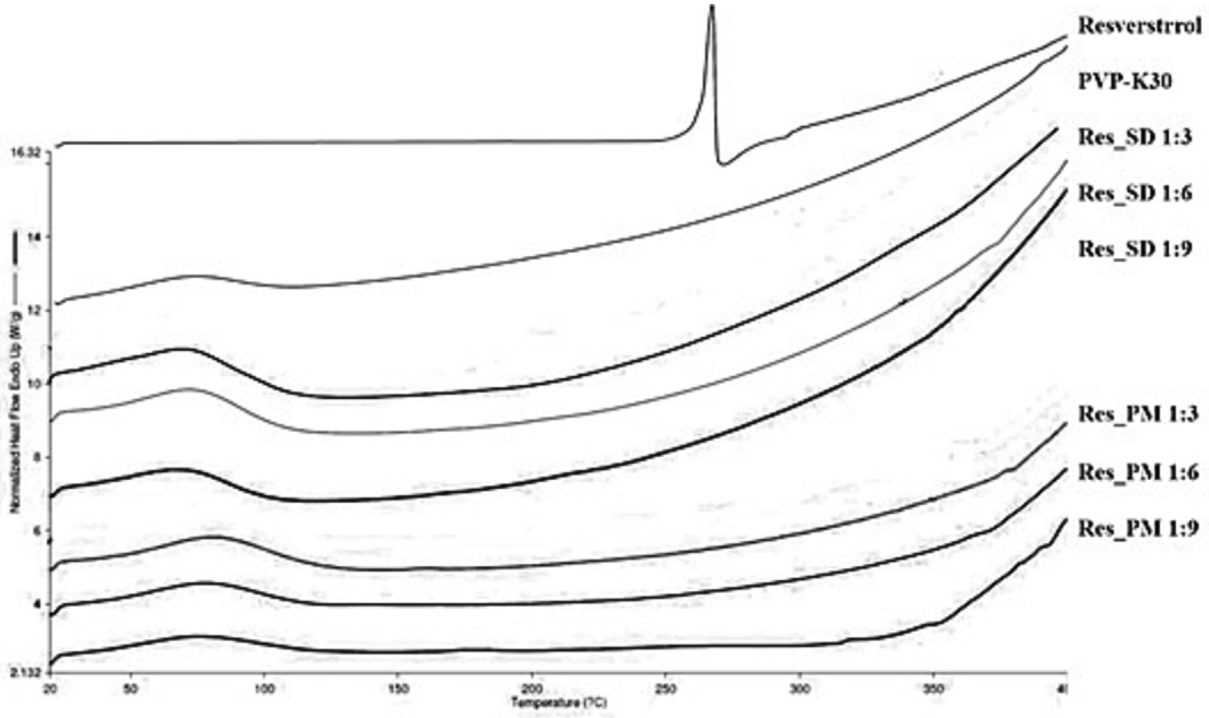

Fig. 2. DSC thermograms of resveratrol, PVP-K30, resveratrol solid dispersion (Res_SD) and resveratrol physical mixture (Res_PM).

the content of chitosan, PVA, crosslinking agent and resveratrol. SPH density decreased by approximately 50 % on increasing the concentration of chitosan and PVA in the starting co-solution from 0.5 % to 2 % (Table 3). This behavior may be explained by the increased strength of the gel network with increasing polymer content, which resists expansion by gas generation. The decrease in hydrogel density from 0.542 to 0.112 g/mL with increasing glyoxal solution addition (crosslinker) may be similarly explained. The increase in Res_SD loaded SPH density from 0.202 to 0.501 g/mL reflected the increased content of SD.

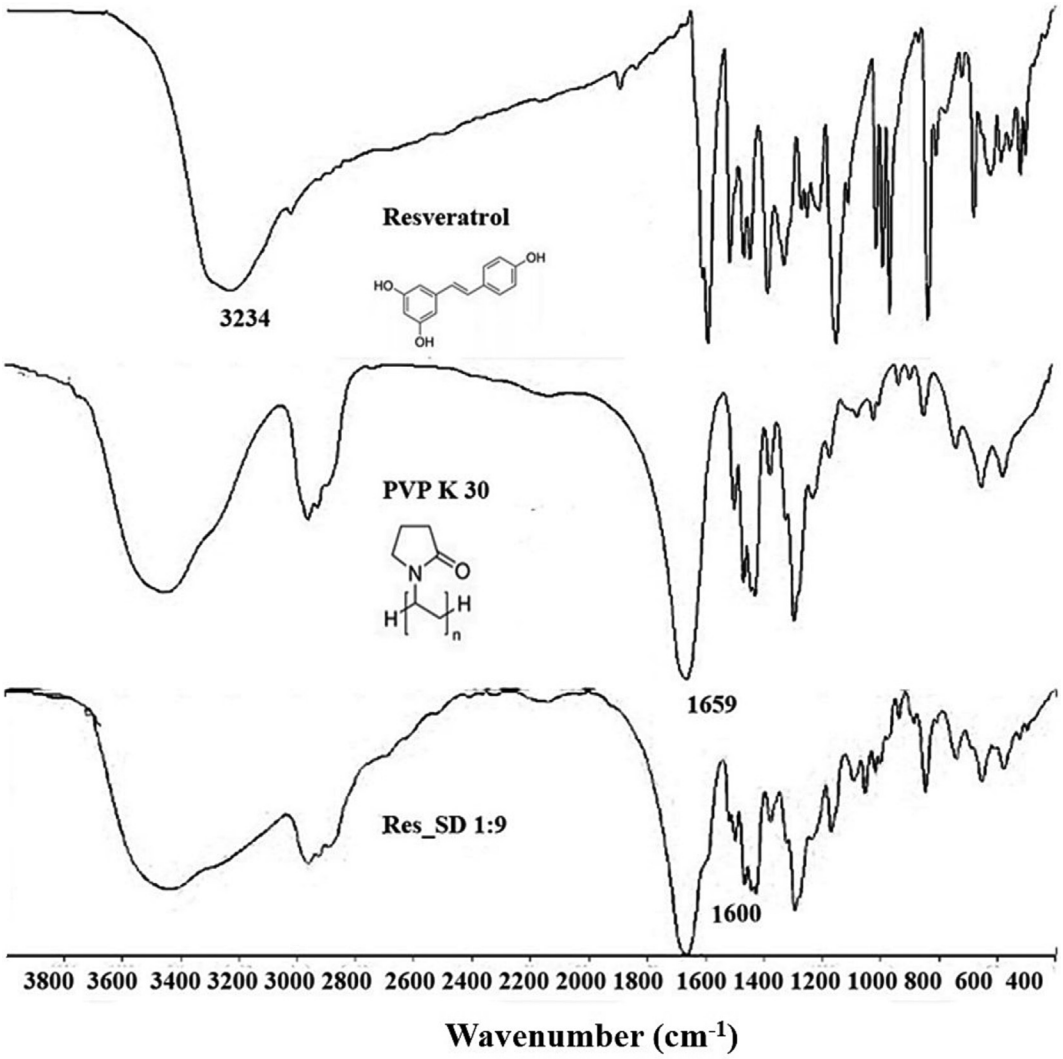

Fig. 3. FT-IR spectra of resveratrol, PVP-K30, and resveratrol solid dispersion (Res_SD).

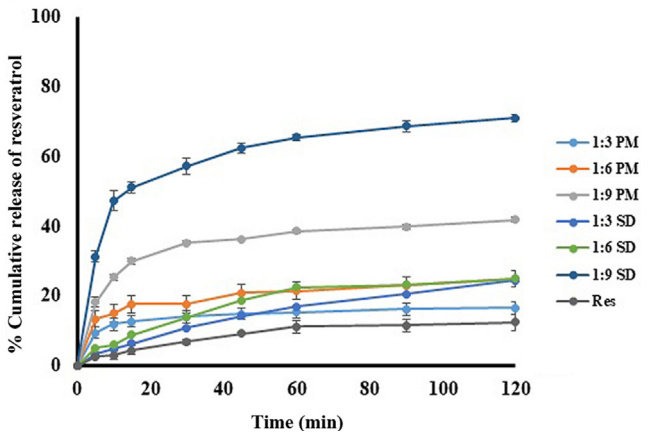

Fig. 4. Dissolution of resveratrol, resveratrol solid dispersion (Res_SD) and resveratrol physical mixture (Res_PM) in 0.1 N HCl, pH 1.2, 37 °C.

3.2.3. Resveratrol encapsulation efficiency (%EE)

In general the Res_SD loaded SPHs exhibited high resveratrol encapsulation efficiency in excess of 75 % within a maximum of 90 % (Table 3). Lower % EE was recorded for formualtions produced using low concentration (0.5 %) chitosan solution (F1) and high (1 %) glyoxal solution content (F12). The lower concentration of chitosan in the starting co-solution with PVA is expected to result in a decrease in viscosity, which favours sedimentation of Res_SD, resulting in decreased entrapment within the hydrogel. The effect of the higher content of glyoxal crosslinking solution in reducing encapsulation of Res_SD is unclear but may also be explained by a reduction in viscosity of the chitosan/PVA co-solution which would increase sedimentation of Res_SD.

3.2.4. Compressive strength measurements

Effective functioning of Res_SD SPH as gastro-retentive drug delivery system must be able to withstand the pressure exerted during gastric contraction. The compressive strength of Res_SD loaded SPH was found to be influenced by chitosan and PVA content, crosslinker concentration and Res_SD loading (Fig. 6). Moreover, the structural integrity of hydrogels prepared using chitosan solution concentration 1 % w/v was maintained during exposure to simulated gastric fluid for 12 h. The maximum compressive load sustained by Res_SD loaded SPH increased significantly from 60 to 375 g when the concentration of chitosan in the formulation increased from 0.5 % to 2 % (Table 3) with a major increase occurring for SPH prepared using 1.5 % chitosan solution. Similar findings were reported previously (Akakuru and Isiuku,

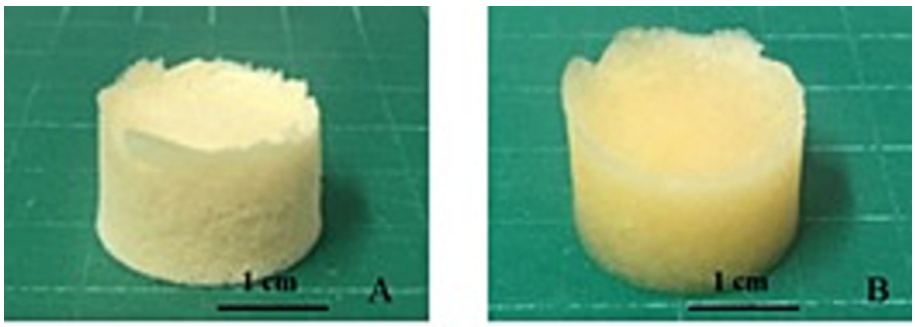

Fig. 5. Macroscopic features of resveratrol solid dispersion loaded superporous hydrogel (F2) in the dried state (A) and swollen condition following immersion in 0.1 N HCl state.

Table 3
Characteristics of superporous hydrogels loaded with resveratrol solid dispersion (Res_SD SPH).

Formulation No.	Weight (mean ± S. D.)	Density (g/mL)	Encapsulation efficiency (%)
Effect of chitosan content			
F1	210.20 ± 1.56	0.457 ± 0.016	68.18 ± 3.54
F2	217.85 ± 0.35	0.202 ± 0.009	75.57 ± 1.04
F3	230.77 ± 0.62	0.211 ± 0.018	81.70 ± 0.39
F4	272.67 ± 2.92	0.165 ± 0.058	84.94 ± 0.87
Effect of PVA content			
F5	190.80 ± 2.91	0.619 ± 0.128	78.98 ± 0.07
F6	217.85 ± 0.35	0.202 ± 0.009	75.57 ± 1.04
F7	221.93 ± 5.24	0.261 ± 0.012	85.01 ± 1.76
F8	253.07 ± 5.96	0.262 ± 0.012	90.27 ± 0.71
Effect of glyoxal solution			
F9	219.60 ± 4.21	0.542 ± 0.011	82.81 ± 1.50
F10	209.60 ± 5.40	0.202 ± 0.009	75.57 ± 1.04
F11	217.85 ± 0.35	0.263 ± 0.012	78.71 ± 2.06
F12	256.93 ± 3.86	0.112 ± 0.002	64.35 ± 4.23
Effect of Res_SD content			
F13	217.85 ± 0.35	0.202 ± 0.009	75.57 ± 1.04
F14	282.95 ± 0.15	0.250 ± 0.015	75.11 ± 1.27
F15	399.23 ± 4.74	0.387 ± 0.039	75.84 ± 1.15
F16	461.80 ± 4.50	0.501 ± 0.049	77.28 ± 1.67

density of gastric content = 1.004 g/cm^3.

2017). Increases in compressive strength from 100 to 250 g were recorded on raising the PVA concentration of the starting co-solution from 0 to 2 % although to a lesser degree than observed for chitosan. This behavior may be explained by the higher network strength resulting from the increased polymer content of the hydrogel and the intermolecular interaction (physical cross-links/entanglements) between chitosan and PVA (Kim et al., 2012; Akakuru and Isiuku, 2017). Hydrogels produced without crosslinking agent displayed expectedly low compressive strength (20.3 g/cm^2) whereas 10 fold increase following added crosslinking agent. Increases in Res_SD loading from 100 to 400 mg resulted in more than doubling of the hydrogel compressive strength due to a particulate reinforcement effect.

3.2.5. Water absorption studies

Water absorption studies carried out in simulated gastric fluid revealed rapid, large scale fluid uptake, typically around 1500 % weight gain, followed by maintenance of the equilibrium state over 60 min (Fig. 7). The rapid fluid uptake suggests that the controlling mechanism is capillary action rather than simple absorption (Chen et al., 2000; Chavda et al., 2009). The formation of hydrogen bonds between water molecules and hydrophilic functional groups (–NH_2) and hydroxyl groups (–OH) in the chitosan chains is expected to promote fluid entry into the hydrogel network (Correlo et al., 2007; Chavda and Patel, 2010). Another, possible mechanism to promote the swelling ratio is the cationization of amine groups in acidic SGF condition (Kim et al., 2003; Ahmadi et al., 2015). Interestingly, the acidic environment of SGF results in ionization of amine groups in the chitosan macromolecules to ammonium ions (NH_3^+), which result in repulsive forces between polymer molecules, and increase the void space for fluid uptake.

SPH prepared using low chitosan concentration solution of 0.5 and 1 % resulted in higher fluid uptake to 1400 % compared with SPH featuring higher chitosan content (approximately 800 % weight gain) as shown in Fig. 7(a). This behavior may be explained by the higher strength of the gel network, resisting expansion (Qiu and Park, 2003; Chavda et al., 2013; Ahmadi et al., 2015). The increase of PVA content in the SPH as represented in Fig. 7(b) resulted in similar fluid absorption behavior to that of chitosan content. The effect of the amount of Res_SDs and glyoxal were also test as illustration in Fig. 7(c) – 7(d), respectively.

The extent of SGF uptake by Res_SD-loaded SPH decreased significantly as the concentration of crosslinking agent increased, in line with the increased rigidity and lower expansion capacity of the hydrogel network. SPHs prepared in the absence of glyoxal solution and exposed to SGF resulted in a mean weight gain of 2300 % but samples collapsed during testing. Fluid uptake of cross-linked SPH samples was restricted to weight gains between 1000 and 1500. The increase in Res_SD content of the SPH from 100 mg to 300 mg resulted in a 50 % reduction in fluid uptake which may be explained by the reinforcing effect of the drug particles on the hydrogel matrix, which restricts expansion.

3.2.6. SEM

The pore sizes of SPHs are generally in the range of a few hundred micrometers. The appropriate pore size was attributed to fast and high water retention with suitable mechanical strength. The internal structure of freeze-dried SPHs exhibited an extensive interconnected pore structure with pore size of approximately 150 μm (Fig. 8). The large surface area and pore interconnectivity evident within the SPH helps explain the rapid fluid uptake by these materials by capillary action (El-Said et al., 2016).

3.2.7. In vitro release of resveratrol from superporous hydrogels

The resveratrol release profiles for Res_SD loaded SPH typically exhibited an initial phase of rapid release over the first two hours exposure to SGF followed by gradual release over the remaining 10 h (Fig. 9). Various factors are known to affect drug release including drug solubility, interaction between drug and polymer and swelling ratio. The content of chitosan and PVA in the SPH was found to exert a significant effect on resveratrol release. The use of high chitosan solution concentrations of 1.5 and 2 % were found to restrict resveratrol release to below 40 % during 12 h exposure to SGF, indicating poor delivery efficiency. In comparison, lower chitosan solution concentrations of 0.5 and 1 % gave rise to

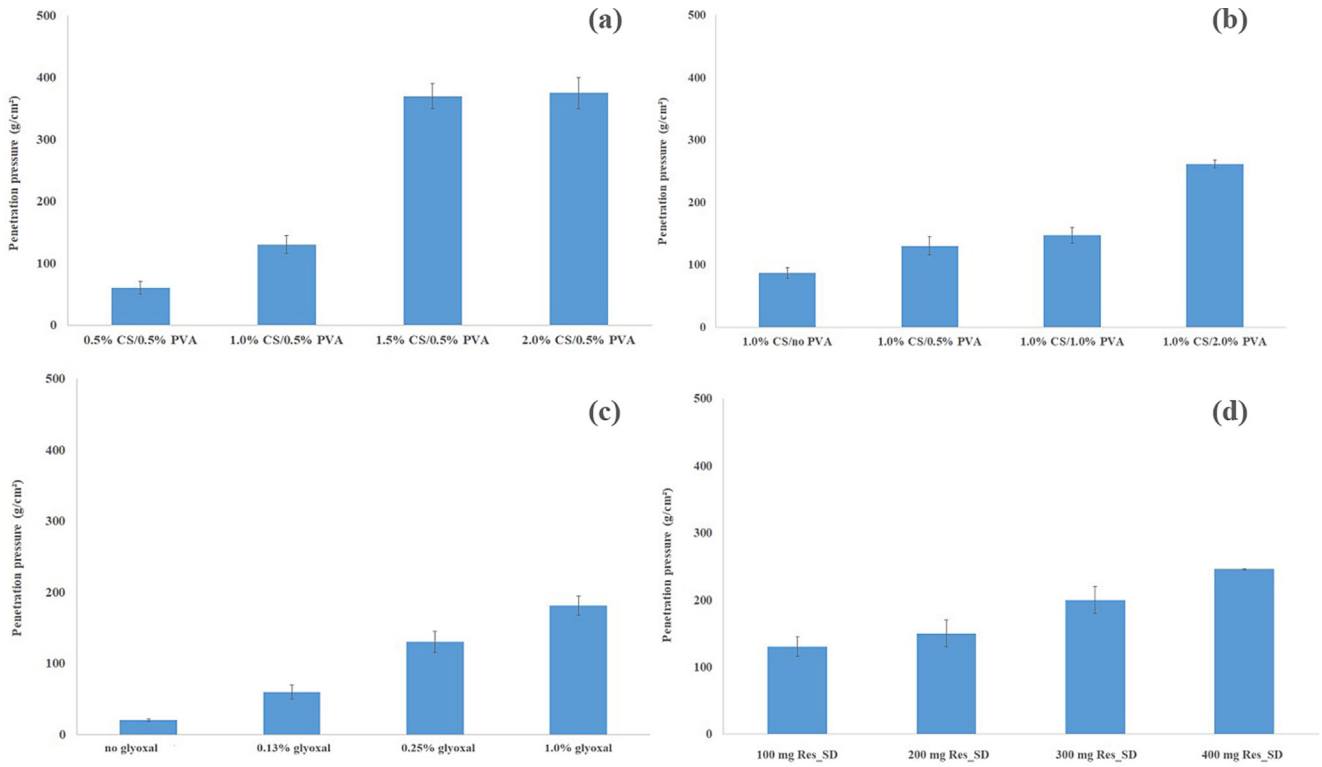

Fig. 6. The compressive strength at different % of chitosan (a), PVA (b), glyoxal solution (c) and the amount of Res_SD (d).

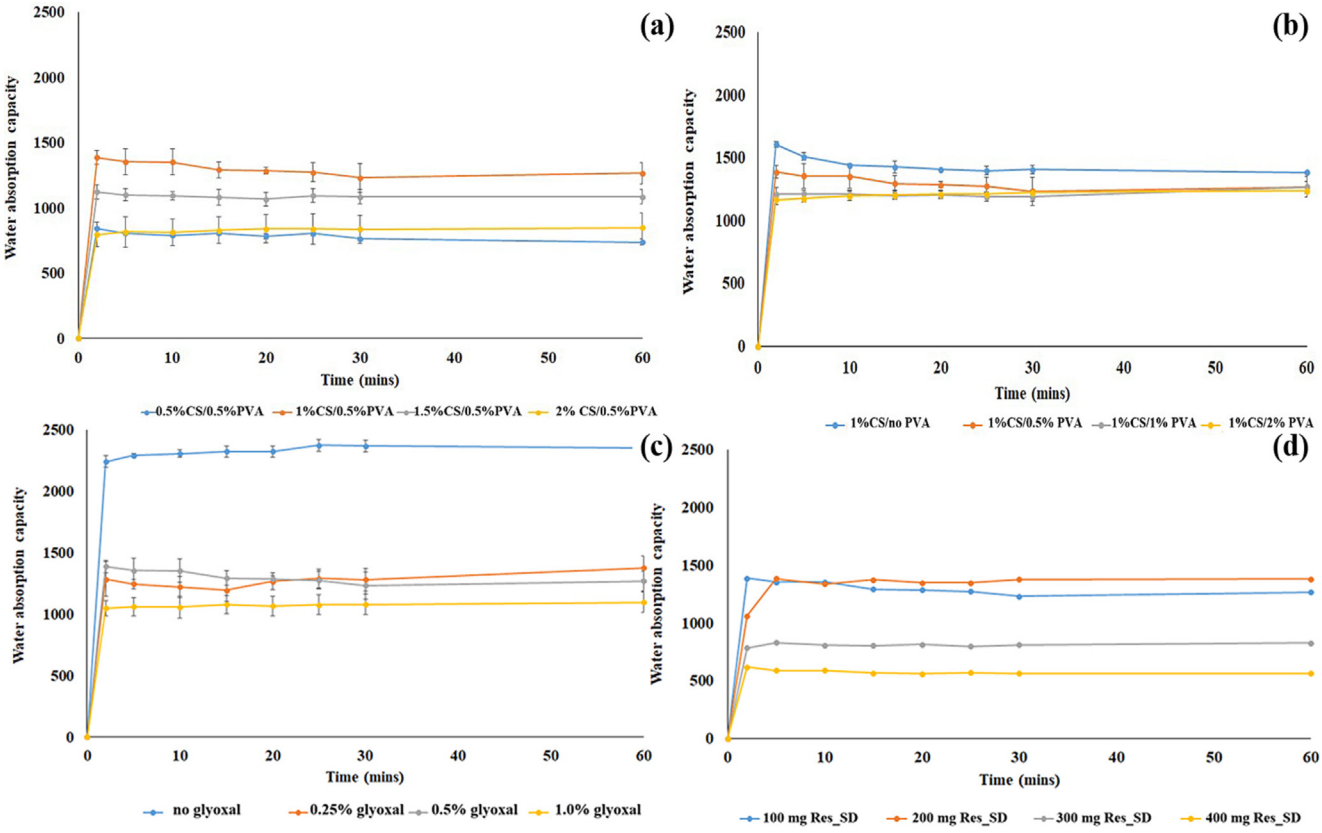

Fig. 7. Water absorption capacity of Res_SD SPHs prepared using varyting amounts of chitosan (a), PVA (b), glyoxal solution (c), and Res_SDs (d).

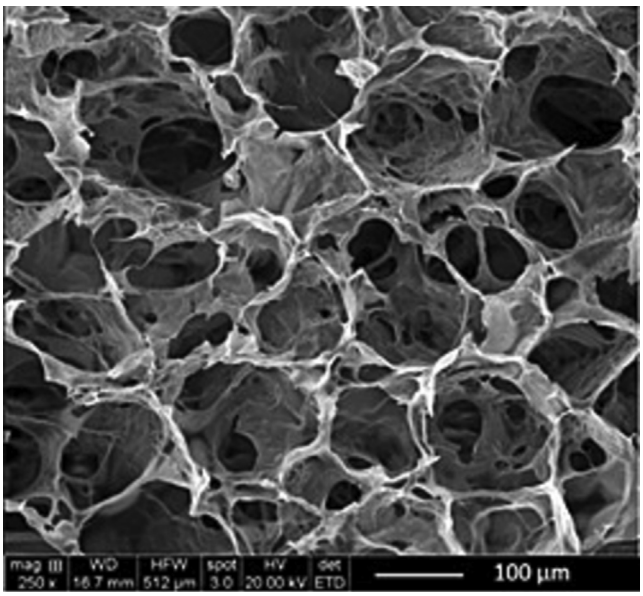

Fig. 8. Internal structure of dried superporous hydrogel loaded with resveratrol solid dispersion (F2).

high resveratrol delivery efficiency of 80 %. Increases in concentration of the PVA solution used to prepare the SPH from zero to resulted in a reduction of resveratrol delivery from 100 to around 70 % (Fig. 9B) although the effect was less marked than observed for increasing content of chitosan in the SPH. Almost complete release of resveratrol (90 %) occurred rapidly from non-crosslinked SPH preparations during the first 2 h exposure to SGF (Fig. 9C) and increasing the glyoxal solution from 0.025 to 1 % v/v had little effect on the release profile or the amount of resveratrol released (79–85 % in 12 h). Contrary to expectations, increasing the content of Res_SD in the SPH from 100 to 300 mg was found to reduce the cumulative release of the phenol from around 70 to 80 % during exposure to SGF for 12 h, whereas complete release was achieved in 8 h when the Res_SD content was set at 200 mg. Higher drug release obtained for 200 mg Res_SD in Fig. 9. The pattern of drug release profiles obtained for SPHs was consistent with their fluid absorption behavior in that hydrogels exhibiting a higher fluid absorption achieved higher % drug release. Based on the above findings of > 90 % resveratrol delivery in SGF, formulaiton F2 prepared using 1 % w/v chitosan solution concentration, 0.5 %w/v PVA solution concentration, 0.13 % v/v glyoxal solution concentration and 200 mg Res_SD was considered to be highly advantageous for gastro-retentive delivery of resveratrol.The release profiles of F2 was also shown initially burst release and followed by prolonged release over 12 h. These pattern represent to the release of drug on the surface of SPHs in the first phase and the diffusion and erosion of SPHs in the second phase. After fitting with the various kinetic models, the release of drug can be explained by Krosmeyer-Peppas model that indicated both diffusion and erosion mechanisms (R^2 = 0.999) (Bhalla and Nagpal, 2013).

3.2.8. *In vitro* degradation kinetics of SPHs

Mass loss of Res_SD SPH in the *in vivo* environment of the stomach is expected to be caused by both mechanical forces and chemical/enzymatic hydrolysis of the polymer chains (Qiu and Park, 2003). The mass remaining profiles recorded for Res_SD SPH during exposure to SGF (Fig. 10) essentially mirrored in reverse the resveratrol release profile presented in Fig. 9. In general, rapid

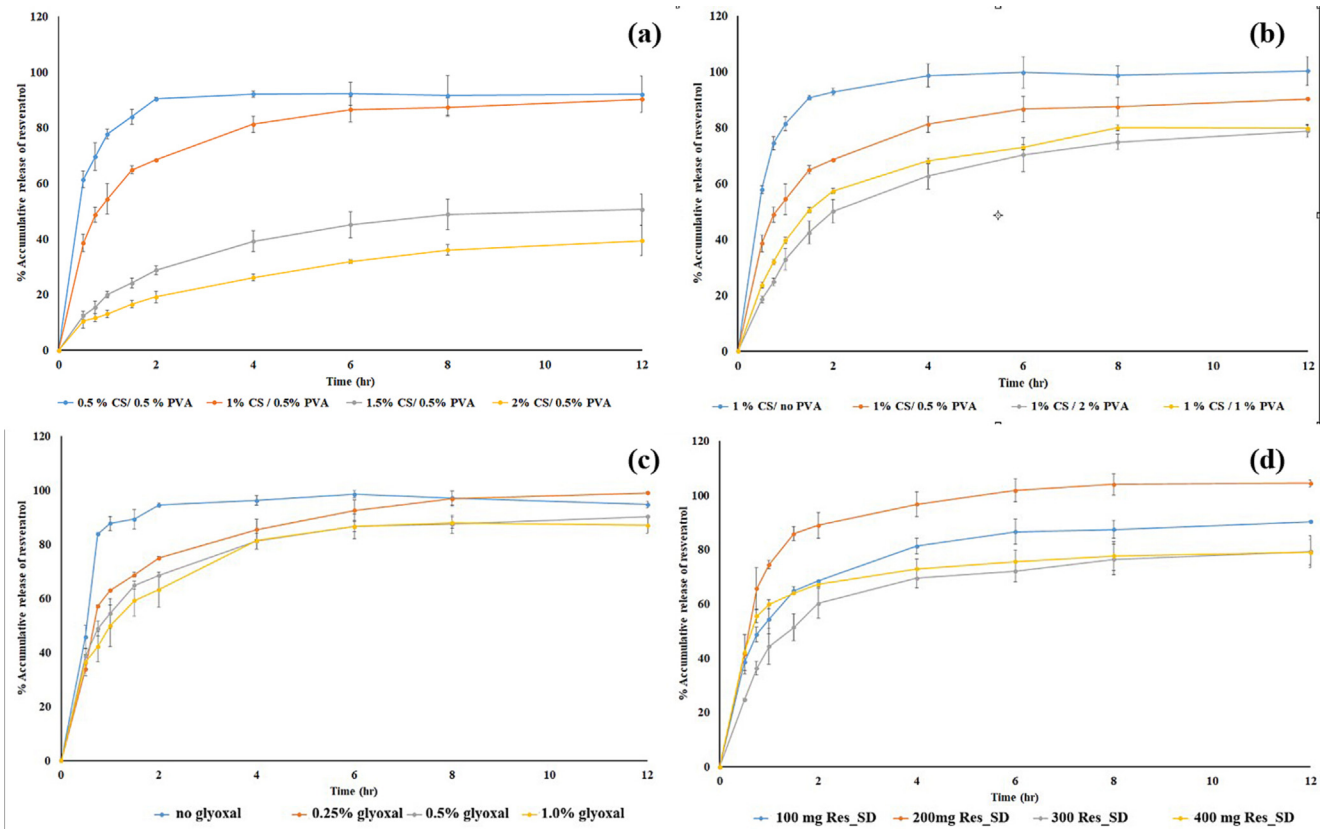

Fig. 9. Cumulative release of resveratrol (% w/w) from superporous hydrogels loaded with resveratrol solid disperisons (Res_SD SPH) in simulated gastric fluid. Effect of chitosan solution concentration (a), PVA solution concentration (b), glyoxal solution (c) and Res_SD content (d) used for SPH preparation.

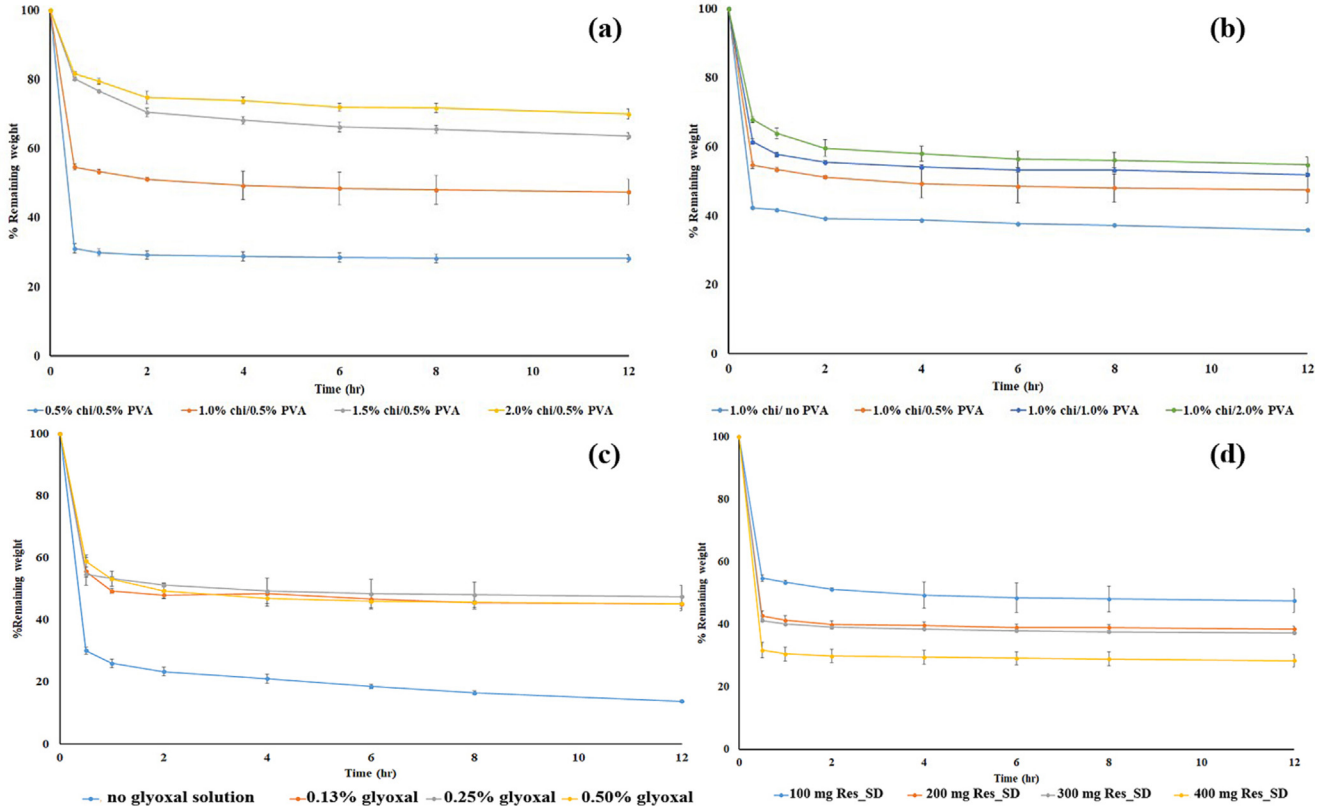

Fig. 10. Mass remaining profiles of Res-SD SPH in simulated gastric fluid. Effect of chitosan solution concentration (a), PVA solution concentration (b), glyoxal solution (c) and Res-SD content (d) used for Res-SD SPH preparation. Data are expressed as the mean ± SD of three experiments.

sample mass loss was evident during the first 30 min and the rate of mass loss plateaued after 2 h. This behavior may be explained by dissfuion of resveratrol molecules and polymeric macromoleculs (chitosan, PVA, PVP) from the hydrogel matrix, probably facilitated by acid hydrolysis of chitosan chains. As discussed above (section 3.2.5) in relation to resveratrol delivery, SPH mass loss is strongly and directly related to the fluid absorption characteristics of the SPHs.

3.2.9. In vitro cytotoxicity and anti-inflammatory properties of superporous hydrogels loaded with Res_SD

MTT assay and anti-NO test were employed using AGS and RAW264.7 cells, respectively. Resveratrol has been reported previously to exhibit anti-cancer activity against gastric cells (Yang et al., 2018). No significant difference was measured between IC50 values of resveratrol loaded SPH (99.3 ± 0.9 μg/mL) and non-formulated resveratrol (82.8 ± 0.5 μg/mL) was measured ($p > 0.05$) (Table 4), indicating the phenol maintained anticanceractivity following formulation. Additionally, the SPH carrier (blank) displayed very low toxicity against AGS cells (IC50 value 558.9 ± 0.5 μg/mL) indicating that the hydrogel did not inhibit the activity of resveratrol. The viability of AGS cells following exposure to increasing concentrations of test samples (5–200 μg/mL) for 24 h is presented in Fig. 11. Non-formulated resveratrol produced the highest cytotoxic effect against AGS cells, resulting in a maximum decrease in cell viability of 90 %. Res_SD loaded SPHs Formulation F2 produced a gradual, concentration-dependent reduction in cell viability of around 70 % with increasing resveratrol concentration. However, resveratrol solid dispersion (Res_SD)

Table 4
Assay of anticancer and anti-inflammatory activity of a) superporous hydrogel loaded with resveratrol solid dispersion b) non-formulated resveratrol and c) blank superporous hydrogel.

Test sample	Cytotoxicity assay IC_{50} (μg/mL)	Anti-NO assay IC_{50} (μg/mL)
Res_SD SPH	99.3 ± 0.9	7.5 ± 0.8
Blank SPH	558.9 ± 0.5	238.1 ± 1.2
Resveratrol	82.8 ± 0.5	6.1 ± 0.5
Indomethacin	–	6.9 ± 0.8

*Statistical significance, $p < 0.05$.
[a] Each value represents the mean ± S.D. of four determinations.

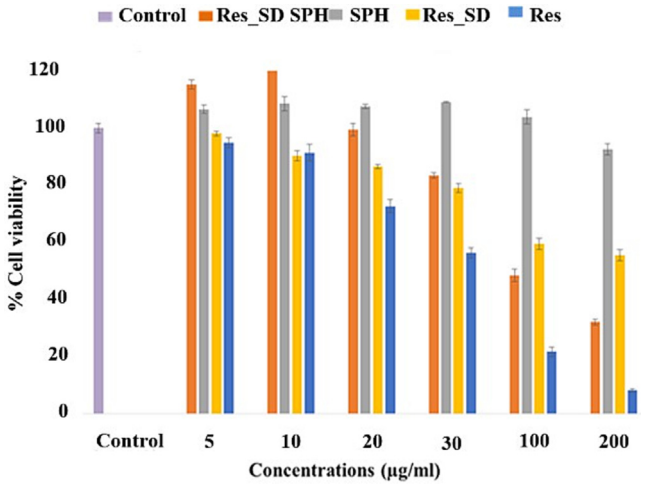

Fig. 11. The viability of human gastric epithelial (AGS) cells following exposure for 24 h to increasing concentrations of superporous hydrogel loaded with resveratrol solid dispersion (Res_SD SPH) (a), blank superporous hydrogel (SPH)(b), resveratrol solid dispersion (Res_SD) (c) and non formulated resveratrol (Res) (d). Data represented as mean ± S.D. (n = 4).

resulted in a smaller reduction in cell viability of 40 % at the highest phenol concentration (200 μg/mL). The reasons for the reduced cytoxicity of Res_SD SPH and Res_SD preparations relative to non-formulated resveratrol are unclear since complete release of resveratrol is expected during the 24 h time period of cell exposure. One explanation may involve the increase in % cell viability recorded for the blank hydrogel and resveratrol–containing hydrogels at low loadings (5–10 μg/mL) in comparison with the blank hygrogel. This result indicates an effect of the phenol itself on cell growth.

3.2.10. Anti-inflammatory activity

Healing of gastric ulcers is promoted by administration of anti-inflammatory therapeutics. Resveratrol has been reported to exert anti-inflammatory effects in LPS-stimulated RAW264.7 cells in a dose-dependent manner by down-regulating the expression of inducible nitric oxide synthase (iNOS) and interleukin-6 (IL-6) and phosphorylation of nuclear factor-κB (NF-κB)(Yang et al., 2018; Pannu and Bhatnagar, 2019). Superporous hydrogel loaded with Res_SD (Formulation F2) was found to strongly inhibit NO production by murine macrophage-like RAW264.7 cells (IC_{50} 7.5 ± 0.8 μg/mL). Importantly, the potent anti-inflammatory effect of non-formulated resveratrol (IC_{50} 6.1 ± 0.5 μg/mL) in comparison with the NSAIDs indomethacin (IC_{50} 6.9 ± 0.8 μg/mL), was largely maintained following incorporation in the hydrogel.

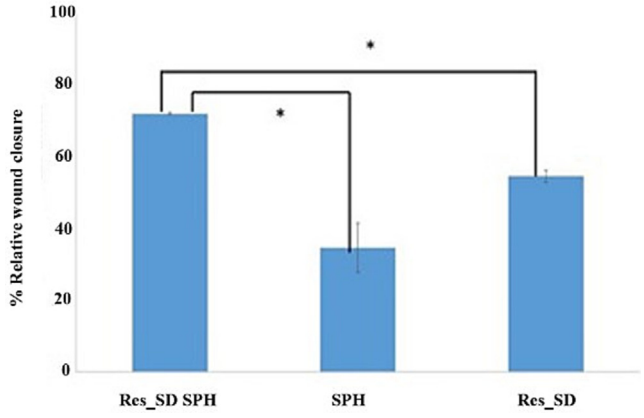

Fig. 12. The % relative wound closure induced in the cell monolayer scratch healing model using superporous hydrogel loaded with resveratrol solid dispersion (Res_SD SPH), blank hydrogel (SPH) and resveratrol solid dispersion (Res_SD). Data presented as mean ± S.D. Statistically significant differences were accepted at p values < 0.05 (*).

3.2.11. Wound healing assay

As mentioned in Section 3.2.9, superporous hydrogels loaded with low concentrations (5–10 μg/mL) of Res_SD were found to exert a proliferative effect on gastric epithelial cells in culture and are therefore of potential benefit for treating lesions in the gastrointestinal tract (Solmaz et al., 2009; Yang et al., 2018). The scratch wound healing assay was performed using monolayer AGS cells exposed to test samples for 24 h. As shown in Fig. 12, superporous hydrogel loaded with Res_SD (Formulation F2) significantly increased % wound closure (72 %) in comparison with blank hydrogel (30 %) and Res_SD (55 %). In addition, the cell migration pictures of Res_SD loaded SPH in comparison with Res_SD and blank SPH are also presented in Fig. 13. It thus appears that a combination of the phenol compound and superporous hydrogel based on chitosan and polyvinyl alcohol is recommended to maximize wound healing potential.

4. Conclusions

The prepared SPH systems based on chitosan and polyvinyl alcohol merging with solid dispersion technology were found to enhance solubility, the gastric residence time and prolong the release of resveratrol. The hydrogels exhibited rapid absorption of simulated gastric fluid while maintaining structural integrity for 12 h. The SPH also acted as a suitable carrier for maintaining the relese of drug in the stomach. Additionally, the resveratrol loaded hydrogels exhibited anti-cancer and anti-inflammatory activity in cell cultures including wound healing capacity at low resveratrol content. These findings illustrated the potential use of SPH based formulations for stomach-specific delivery of resveratrol and other poorly water-soluble compounds.

Declaration of Competing Interest

The authors declare that they have no known competing financial interests or personal relationships that could have appeared to influence the work reported in this paper.

Acknowledgments

This study was financial supported by the Faculty of Pharmaceutical Sciences, Prince of Songkla University and The Thailand Research Fund under the Royal Golden Jubilee Ph.D. Program (PHD/0087/2559). We would like to thank Prof.Allan Coombes for assistance with English editing of the manuscript and scientific/technical advice.

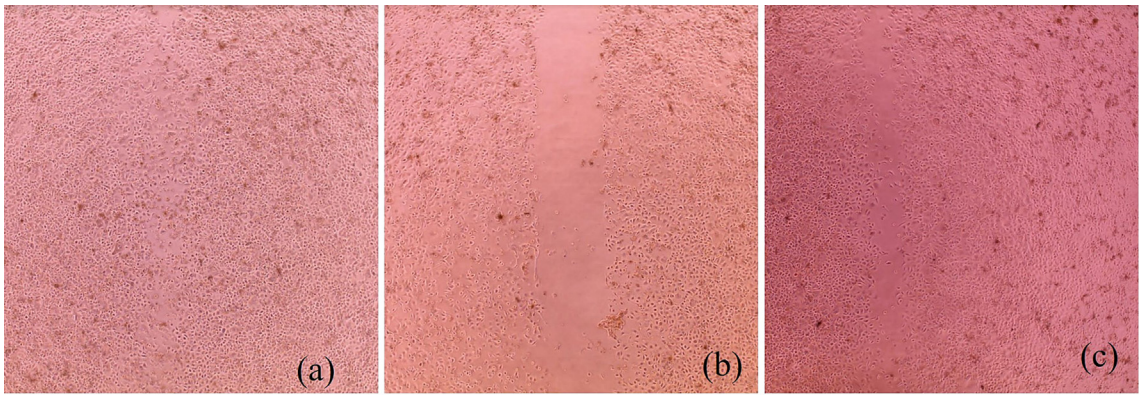

Fig. 13. The cell migration of superporous hydrogel loaded with resveratrol solid dispersion Res-SD SPH (a), blank hydrogel (SPH) (b) and resveratrol solid dispersion (c) at 5 μg/mL for 48 h.

References

Afifi, S., 2015. Solid dispersion approach improving dissolution rate of stiripentol: a novel antiepileptic drug. Iran J. Pharm. Res. 14, 1001–1014.

Ahmadi, F., Oveisi, Z., Samani, S.M., Amoozgar, Z., 2015. Chitosan based hydrogels: characteristics and pharmaceutical applications. Res. Pharm. Sci. 10, 1–16.

Akakuru, O., Isiuku, B., 2017. Chitosan hydrogels and their glutaraldehyde-crosslinked counterparts as potential drug release and tissue engineering systems-synthesis, characterization, swelling kinetics and mechanism. J. Phys. Chem. Biophys. 7, 1–7. https://doi.org/10.4172/2161-0398.1000256.

Almeida, T.C., Seibert, J.B., Almeida, S.H.S., Amparo, T.R., Teixeira, L.F.M., Barichello, J. M., Postacchini, B.B., Santos, O.D.H., da Silva, G.N., 2020. Polymeric micelles containing resveratrol: development, characterization, cytotoxicity on tumor cells and antimicrobial activity. Braz. J. Pharm. Sci. 56, e1841.

Baghel, S., Cathcart, H., O'Reilly, N.J., 2016. Polymeric amorphous solid dispersions: A review of amorphization, crystallization, stabilization, solid-state characterization, and aqueous solubilization of biopharmaceutical classification system Class II drugs. J. Pharm. Sci. 105, 2527–2544. https://doi.org/10.1016/j.xphs.2015.10.008.

Bhalla, S., Nagpal, M., 2013. Comparison of various generations of superporous hydrogels based on chitosan-acrylamide and in vitro drug release. ISRN Pharm. 2013,. https://doi.org/10.1155/2013/624841 624841.

Boontawee, R., Issarachot, O., Kaewkroek, K., Wiwattanapatapee, R., 2022. Foldable/expandable gastro-retentive films based on starch and chitosan as a carrier for prolonged release of resveratrol. Curr. Pharm. Biotechnol. 23, 1009–1018.

Chavda, H., Modhia, I., Mehta, A., Patel, R., Patel, C., 2013. Development of bioadhesive chitosan superporous hydrogel composite particles based intestinal drug delivery system. Biomed. Res. Int. 2013,. https://doi.org/10.1155/2013/563651 563651.

Chavda, H.V., Patel, C., Karen, H., 2009. Preparation and characterization of chitosan-based superporous hydrogel composite. J. Young. Pharm. 1, 199. https://doi.org/10.4103/0975-1483.57064.

Chavda, H., Patel, C., 2010. Chitosan superporous hydrogel composite-based floating drug delivery system: A newer formulation approach. J. Pharm. Bioallied. Sci. 2, 124–131. https://doi.org/10.4103/0975-7406.67010.

Chen, J., Blevins, W.E., Park, H., Park, K., 2000. Gastric retention properties of superporous hydrogel composites. J. Control. Release 64, 39–51. https://doi.org/10.1016/s0168-3659(99)00139-x.

Correlo, V.M., Pinho, E.D., Pashkuleva, I., Bhattacharya, M., Neves, N.M., Reis, R.L., 2007. Water absorption and degradation characteristics of chitosan-based polyesters and hydroxyapatite composites. Macromol. Biosci. 7, 354–363. https://doi.org/10.1002/mabi.200600233.

El-Said, I.A., Aboelwafa, A.A., Khalil, R.M., ElGazayerly, O.N., 2016. Baclofen novel gastroretentive extended release gellan gum superporous hydrogel hybrid system: *in vitro* and *in vivo* evaluation. Drug Deliv. 23, 101–112. https://doi.org/10.3109/10717544.2014.905654.

Farag, M.M., Louis, M.M., Badawy, A.A., et al., 2022. Drotaverine hydrochloride superporous hydrogel hybrid system: a gastroretentive approach for sustained drug delivery and enhanced viscoelasticity. AAPSPharmSciTech. 23, 124. https://doi.org/10.1208/s12249-022-02280-2.

Fitriani, L., Haqi, A., Zaini, E., 2016. Preparation and characterization of solid dispersion freeze-dried efavirenz - polyvinylpyrrolidone K-30. J. Adv. Pharm. Technol. Res. 7, 105–109. https://doi.org/10.4103/2231-4040.184592.

Gao, P., Shi, Y., 2012. Characterization of supersaturatable formulations for improved absorption of poorly soluble drugs. AAPS J. 14, 703–713. https://doi.org/10.1208/s12248-012-9389-7.

Gupta, N.V., Shivakumar, H.G., 2010. Preparation and characterization of superporous hydrogels as gastroretentive drug delivery system for rosiglitazone maleate. Daru 18, 200–210.

Huang, Y., Dai, W.G., 2014. Fundamental aspects of solid dispersion technology for poorly soluble drugs. Acta Pharm. Sin. B 4, 18–25. https://doi.org/10.1016/j.apsb.2013.11.001.

Jaisamut, P., Wiwattanawongsa, K., Wiwattanapatapee, R., 2017. A Novel self-microemulsifying system for the simultaneous delivery and enhanced oral absorption of curcumin and resveratrol. Planta Med. 83 (5), 461–467.

Kaewkroek, K., Petchsomrit, A., Wira Septama, A., Wiwattanapatapee, R., 2022. Development of starch/chitosan expandable films as a gastroretentive carrier for ginger extract-loaded solid dispersion. Saudi Pharm. J. 30, 120–131. https://doi.org/10.1016/j.jsps.2021.12.017.

Kaewnopparat, N., Kaewnopparat, S., Jangwang, A., Maneenaun, D., Chuchome, T., Panichayupakaranant, P., 2009. Increased solubility, dissolution and physicochemical studies of curcumin-polyvinylpyrrolidone K-30 solid dispersions. World Acad. Sci. Eng. Technol. 31, 225–230.

Kerdsakundee, N., Mahattanadul, S., Wiwattanapatapee, R., 2015. Development and evaluation of gastroretentive raft forming systems incorporating curcumin-Eudragit® EPO solid dispersions for gastric ulcer treatment. Eur. J. Pharm. Biopharm. 94, 513–520. https://doi.org/10.1016/j.ejpb.2015.06.024.

Kim, G.O., Kim, N., Kim, D.Y., Kwon, J.S., Min, B.-H., 2012. An electrostatically crosslinked chitosan hydrogel as a drug carrier. Molecules 17, 13704–13711. https://doi.org/10.3390/molecules171213704.

Kim, S.J., Shin, S., Lee, Y.M., Kim, S., 2003. Swelling characterizations of chitosan and polyacrylonitrile semi-interpenetrating polymer network hydrogels. J. Appl. Polym. Sci. 87, 2011–2015. https://doi.org/10.1002/app.11699.

Ko, J.H., Sethi, G., Um, J.Y., Shanmugam, M.K., Arfuso, F., Kumar, A.P., Bishayee, A., Ahn, K.S., 2017. The role of resveratrol in cancer therapy. Int. J. Mol. Sci. 18, 1–36. https://doi.org/10.3390/ijms18122589.

Kumari, P.V.K., Sharmila, M., Rao, Y.S., 2020. Super porous hydrogels: a review. J. Pharm. Res. Int. 32, 153–165.

Kuršvietienė, L., Stanevičienė, I., Mongirdienė, A., Bernatonienė, J., 2016. Multiplicity of effects and health benefits of resveratrol. Medicina (Kaunas) 52, 148–155. https://doi.org/10.1016/j.medici.2016.03.003.

Liang, C.C., Park, A.Y., Guan, J.L., 2007. In vitro scratch assay: a convenient and inexpensive method for analysis of cell migration in vitro. Nat. Protoc. 2, 329–333. https://doi.org/10.1038/nprot.2007.30.

Nayak, A.K., Maji, R., Das, B., 2010. Gastroretentive drug delivery systems: a review. Asian J. Pharm. Clin. Res. 3, 2–10.

Omidian, H., Park, K., 2011. Superporous hydrogels for drug delivery systems, in: Comprehensive biomaterials. Elsevier, pp. 563–576. https://doi.org/10.1016/b978-0-08-055294-1.00044-1.

Omidian, H., Park, K., Rocca, J., 2007. Recent developments in superporous hydrogels. J. Pharm. Pharmacol. 59, 317–327. https://doi.org/10.1211/jpp.59.3.0001.

Panizzon, G.P., Giacomini Bueno, F., Ueda-Nakamura, T., Nakamura, C.V., Dias Filho, B.P., 2019. Manufacturing different types of solid dispersions of BCS class IV polyphenol (Daidzein) by spray drying: Formulation and bioavailability. Pharmaceutics 11 (10), 492. https://doi.org/10.3390/pharmaceutics11100492.

Pannu, N., Bhatnagar, A., 2019. Resveratrol: from enhanced biosynthesis and bioavailability to multitargeting chronic diseases. Biomed. Pharmacother. 109, 2237–2251. https://doi.org/10.1016/j.biopha.2018.11.075.

Payghan, S., 2014. Novel approach in gastroretentive drug delivery system: floating microspheres. Int. J. Pharm. Biol. Sci. Arch. 2, 9–22.

Petchsomrit, A., Sermkaew, N., Wiwattanapatapee, R., 2017. Alginate-based composite sponges as gastroretentive carriers for curcumin-loaded self-microemulsifying drug delivery systems. Sci. Pharm. 85 (11).

Qiu, Y., Park, K., 2003. Superporous IPN hydrogels having enhanced mechanical properties. AAPS PharmSciTech. 4, 406–412.

Sachett, A., Gallas-Lopes, M., Benvenutti, R., Marcon, M., Aguiar, G.P.S., Herrmann, A. P., et al., 2022. Curcumin micronization by supercritical fluid: in vitro and in vivo biological relevance. Ind. Crops. Prod. 177,. https://doi.org/10.1016/j.indcrop.2021.114501 114501.

Sermkaew, N., Wiwattanawongsa, K., Ketjinda, W., Wiwattanapatapee, R., 2013. Development, characterization and permeability assessment based on Caco-2 monolayers of self-microemulsifying floating tablets of tetrahydrocurcumin. AAPS PharmSciTech. 14 (1), 321–331.

Sharma, K.S., Sahoo, J., Agrawal, S., Kumari, A., 2019. Solid dispersions : a technology for improving bioavailability. J. Anal. Pharm. Res. 8 (4), 127–133.

Solmaz, A., Sener, G., Cetinel, S., Yüksel, M., Yeğen, C., Yeğen, B.C., 2009. Protective and therapeutic effects of resveratrol on acetic acid-induced gastric ulcer. Free Radic. Res. 43, 594–603. https://doi.org/10.1080/10715760902977424.

Tran, P., Pyo, Y.C., Kim, D.H., Lee, S.E., Kim, J.K., Park, J.S., 2019. Overview of the manufacturing methods of solid dispersion technology for improving the solubility of poorly water-soluble drugs and application to anticancer drugs. Pharmaceutic. 11, 1–26. https://doi.org/10.3390/pharmaceutics11030132.

Tripathi, J., Thapa, P., Maharjan, R., Jeong, S.H., 2019. Current state and future perspectives on gastroretentive drug delivery systems. Pharmaceutics 11, 1–22. https://doi.org/10.3390/pharmaceutics11040193.

Van den Mooter, G., 2012. The use of amorphous solid dispersions: a formulation strategy to overcome poor solubility and dissolution rate. Drug Discov. Today Technol. 9, e79–e85. https://doi.org/10.1016/j.ddtec.2011.10.002.

Wannasarit, S., Puttarak, P., Kaewkroek, K., Wiwattanapatapee, R., 2019. Strategies for improving healing of the gastric epithelium using oral solid dispersions loaded with pentacyclic triterpene-rich centella extract. AAPS PharmSciTech. 20, 277. https://doi.org/10.1208/s12249-019-1488-7.

Wegiel, L.A., Mauer, L.J., Edgar, K.J., Taylor, L.S., 2013. Crystallization of amorphous solid dispersions of resveratrol during preparation and storage-Impact of different polymers. J. Pharm. Sci. 102, 171–184. https://doi.org/10.1002/jps.23358.

Yang, Z., Xie, Q., Chen, Z., Ni, H., Xia, L., Zhao, Q., Chen, Z., Chen, P., 2018. Resveratrol suppresses the invasion and migration of human gastric cancer cells via inhibition of MALAT1-mediated epithelial-to-mesenchymal transition. Exp. Ther. Med. 1569–1578. https://doi.org/10.3892/etm.2018.7142.

Yang, T., Zhang, J., Zhou, J., Zhu, M., Wang, L., Yan, L., 2018. Resveratrol inhibits interleukin-6 induced invasion of human gastric cancer cells. Biomed. Pharmacother. 99, 766–773. https://doi.org/10.1016/j.biopha.2018.01.153.

Zhang, X., Jiang, A., Qi, B., Ma, Z., Xiong, Y., Dou, J., Wang, J., 2015. Resveratrol protects against Helicobacter pylori-associated gastritis by combating oxidative stress. Int. J. Mol. Sci. 16, 27757–27769. https://doi.org/10.3390/ijms161126061.

Zhang, X., Xing, H., Zhao, Y., Ma, Z., 2018. Pharmaceutical dispersion techniques for dissolution and bioavailability enhancement of poorly water-soluble drugs. Pharmaceutics 10, 1–33. https://doi.org/10.3390/pharmaceutics10030074.